International Journal of Research in Engineering, Science and Management
Volume-2, Issue-12, December-2019
www.ijresm.com | ISSN (Online): 2581-5792

Effect of Zr on Dielectric, Ferroelectric and Impedance Properties of $Na_{0.5}Bi_{0.5}Ti_{0.8}Zr_{0.2}O_3$ Ceramics

Dibakar Panda[1], B. B. Mohanty[2], P. S. Sahoo[3], R. N. P. Choudhary[4]
[1]*Technical Officer-B, Department of Imaging Wing, DRDO, Balasore, India*
[2]*Lecturer, Department of Physics, Betnoti College, Betnoti, India*
[3]*Reader, Department of Physics, North Orissa University, Baripada, India*
[4]*Professor, Department of Physics, Institute of Technical Education & Research, Bhubaneswar, India*

***Abstract*: A polycrystalline orthorhombic compound of Zr-doped Na0.5Bi0.5Ti0.8Zr0.2O3 was prepared by conventional solid state reaction method at high temperature (i.e., at 900˚C). The effect of Zr (0·2) on the structural and microstructural properties of Na0.5Bi0.5Ti0.8Zr0.2O3 was investigated by XRD and SEM. The electrical properties (dielectric, ferroelectric and impedance spectroscopy) were measured in wide range of frequency and temperature. The room temperature X-ray diffraction study assured the evolution of single-phase compound with orthorhombic structure.The dielectric analysis of Na0.5Bi0.5Ti0.8Zr0.2O3 explored over a broad frequency range ($10^3 - 10^6$ Hz) at various temperatures (33˚C - 500˚C) displayed that the dielectric properties of the material are dependent on both frequency and temperature. Dielectric study reveals that the ferro to paraelectric phase transition of the studied compound is a temperature of 268˚C. The nature of the variation of conductivity and value of activation energy in different regions, calculated from the temperature dependence of ac conductivity suggest that the conduction process is of mixed type (i.e., ionic–polaronic and space charge generated from the oxygen ion vacancies).**

***Keywords*: Ceramics, Perovskite Structure, Solid-State Reaction, X-Ray Diffraction, dielectric, impedance, diffuse phase transitions.**

1. Introduction

Since the revelation of barium titanate, BaTiO3, in polycrystalline structure, it has been broadly utilized in different electronic segments, for example, multilayer capacitor (MLCs), positive temperature coefficients of resistivity (PTCR) thermistor, piezoelectric gadget, optoelectronic segments and semiconductors (Morrison et al 2001; Weber et al 2001; Mahajan et al 2009). For MLCs applications, dielectric materials should be electrically protecting (>1010 Ω cm and show high permittivity esteems (> 1000) at room temperature (Morrison et al 2001). Valuable properties for business gadget applications have been generally watched initially in toxic perovskite mixes, for example, PMN–PT, PNN–PZT, PLZT and PZT (Park and Shrout 1997; Fu and Cohen 2000; Mahajan et al 2009). These pieces have a conspicuous detriment of unpredictability and harmfulness of 'lead'. Makers are presently being shunned utilizing materials particularly those containing lead. Subsequently, as of late, inquire about endeavors have been coordinated more towards the improvement of ecological agreeable 'without lead' compositions. Retribution the abovementioned, the ferroelectric oxides of perovskite auxiliary family have primarily been tested for their helpful dielectric [5], electro-optic [6], nonlinear optic [7] pyroelectric [8], piezoelectric [9] properties. An ideal perovskite structure can be spoken to by a general equation as ABO3 where A will be an enormous cation (mono to trivalent) and B is a little cation (a change metal particle). The A particles involve the edges of the 3D square, which is 12 composed, while the B particles sit on the body focus positions inside an oxygen octahedron, which are at the face focus positions. Literature survey disclosed that an abundant of research has been cultivated on perovskite type ferroelectric oxides niobates and tantalates [11]-[13]. We couldn't discover any, however, no work is executed on the auxiliary, dielectric and electrical properties of current compound. Looking to the significance of the material, we have combined and investigated the auxiliary and dielectric properties of another compound having the concoction equation $Na0.5Bi0.5Ti0.8Zr0.2O_3$.

2. Experimental Procedure

A. Material preparation

The stoichiometric ratio of starting chemicals NaCO3 (>99·9%), Bi2O3 (>99·9%), TiO2 (>99·9%) and ZrO2 (>99·9%) were weighed for the composition Na0.5Bi0.5Ti1-xZrxO3 (x = 0.2). The weighed powders were blended mechanically by an agate mortar for about 3 h. The powders were then calcined at optimized temperature and time (900˚C for 12 h) in air condition. The calcined powder thus procured was blended with PVA (poly vinyl alcohol) binder, grinded and were palletized ensuingly (about 10 mm in diameter and 1 - 2 mm thickness) under uniaxial pressure of 4× 10^6 N/m^2. Thereafter the pellets were sintered in air atmosphere at 950˚C

for 12 h. Ultimately the pellets were laminated with high purity silver paint, and then heated at 150˚C for 2 h before executing the electrical measurements.

B. Material characterization

X-ray diffraction (XRD) pattern of the material procured in a vast range of Bragg angle 2θ ($20^0 \leq 2\theta \leq 80^0$) at a scanning speed of 3^0 /min by an X-ray diffractometer (Rigaku, Miniflex) with CuKα radiation (λ = 1.5405 A) at room temperature. The surface morphology of the pellet sample of the material was recorded with a high-resolution scanning electron microscope (SEM: JOEL-JSM model: 5800F). The dielectric characterisation of the sample was prosecuted in the temperature range of 32˚C - 5000˚C and frequency range of 1 kHz to 1 MHz, using a computer-controlled Hioki HiTester LCR meter.

3. Results and discussion

A. Structural and Microstructural Analysis

Figure 1 & 2 shows the XRD pattern of the sample. Ordering of all the peaks of the pattern were done taking their 2θ values by a computer program package, "POWDMULT" [14] in distinct crystal system and cell configuration and are traced to be sharp and solo, which The peaks are discrete from those of ingredients ensuring the evolution of new single-phase compound. On the basis of the best agreement (based on least-squares refinement) between scrutinised (obs) and reckoned (cal) inter planer distance d (i.e., Σ (dobs − dcal) = minimum), an orthorhombic unit cell was selected with lattice parameters: a = 23.6720 (29) Å, b =8.5031 (29) Å, c = 7.5427 (29) Å (estimated standard deviation in parentheses) which are consistence with the reported ones [15].

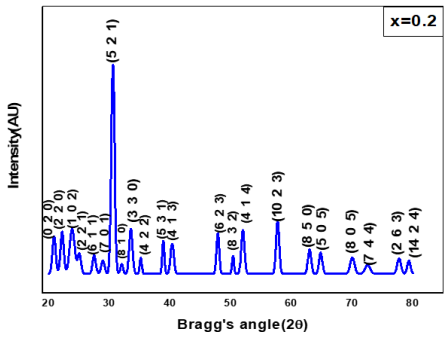

Fig. 1. Room temperature XRD pattern of Na0.5Bi0.5Ti0.8Zr0.2O3 compound.

The coherently average dispersed crystallite size (D) of the compound was computed to be ~ 15 nm using Scherrer's equation; D = 0.89λ/(β1/2cosθhkl), where λ = 1.5405 A and β1/2 = peak width of the reflection at half maxima [16]. The contributions of strain, instrumental error and other unknown effects in the peak broadening have not been taken into board during the crystallite size enumeration. The room temperature SEM micrograph (Figure 2 (left) of the NBTZ compound, confirmed homogenously and non-uniform distribution of the grains over the entire surface of the sample. The grain size evaluated from the histogram Figure 2 (right) is traced to be of 4.9 μm. As expected, the grain size of the sample obtained here is gigantic in comparison to the crystallite size enumerated from Scherrer's equation. Thus, a solo grain has large number of crystallites [17].

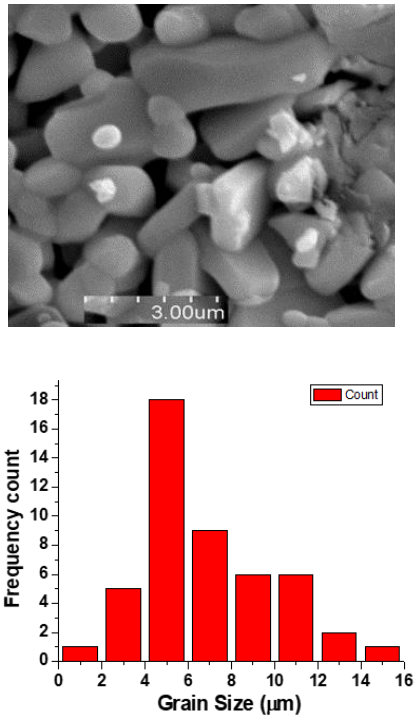

Fig. 2. SEM micrographs and histogram (left) and and histogram (right) of Na0.5Bi0.5Ti0.8Zr0.2O3 compound.

B. Dielectric Analysis

The temperature variety of relative dielectric consistent (εr) at some chose frequencies of compound is demonstrated Figure 3. The plot solidly settled the ferro to paraelectric stage progress at 268˚C. The estimation of εr is small at low temperatures which increments with ascend in temperature. The dielectric constant (εr) at frequencies 10, 50, 100, 500 and 1000 kHz are seen as 255, 245, 220, 185 and 165 respectively at the transition temperature. The variety of tanδ pursues a similar pattern as that of εr. The expansion in the estimation of tanδ might be expected to (I) improvement in the conductivity and (ii) decrease in the commitment of ferroelectric domain wall [18].

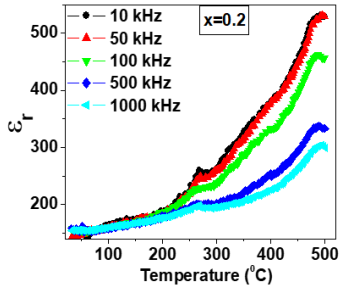

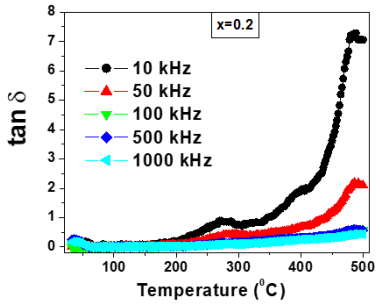

Fig. 3. Variation of εr and tanδ (right) with temperature of Na0.5Bi0.5Ti0.8Zr0.2O3 at some selected frequencies

C. Ac Conductivity Analysis

The ac electrical conductivity (σ_{ac}) is determined utilizing the dielectric information and an empirical connection. σ_{ac} = $\omega \epsilon_r \epsilon_0 \tan\delta$, where ϵ_0 = permittivity of free space and ω = angular frequency. Figure 4 shows the variation of σac as a function of temperature at frequencies 10 and 100 kHz. The nature of the variation (Figure 4) is almost linear over a wide temperature area complying with the Arrhenius relation: $\sigma_{ac} = \sigma_0 \exp(-E_a/k_B T)$ [19], each of charts is divided into two unique regions independently of frequency. Every divided region is characterized by different slopes showing different activation energy. The solid line of figure shows the linear fit. The activation energy calculated from the slope of the curve at different temperatures has been compared in Table 1. Because of the dielectric phase transitions, abnormality in conductivity was observed for the entire compound at temperatures nearly equal to its Curie temperature, which may be because of the dielectric phase transitions. The value of σ_{ac} increases with increase in temperature indicating negative temperature coefficient of resistance (NTCR) behavior. The increase in conductivity is due to the hopping action of the ions because of thermally activated electrons. At high temperature higher value of activation energy indicates that conductivity is for the movement of oxygen vacancies. Activation energy is low at high frequency as compared to that at the low frequency (Table 1). This is because at low frequencies the overall conductivity is the result of hopping of charge carriers over a large distance and at higher frequencies is restricted to only nearest neighbouring defects sites [20].

Table 1
Comparison of activation energy Ea (eV) of Na0.5Bi0.5Ti0.8Zr0.2O3 at two different frequencies in region I, II and III, calculated from σ_{ac} vs. 1/T graphs

Frequency (kHz)	Activation energy E_a (eV)		
	Region I	Region II	Region III
10	0.0558	0.5925	0.7517
100	0.0804	0.5461	0.4502

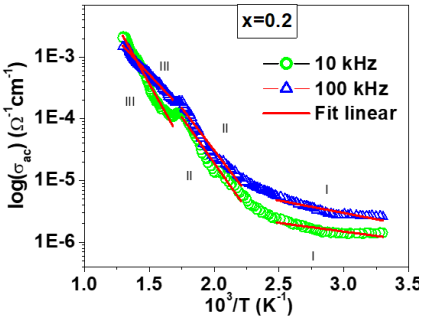

Fig. 4. Variation of σ_{ac} with 1000/T of $Na_{0.5}Bi_{0.5}Ti_{0.8}Zr_{0.2}O_3$ at two selected frequencies

D. Complex immittance spectroscopy

Figure 5 (a and b) & figure 6 represents the variation of imaginary part of impedance (Z'') and modulus as a function of frequency at different temperatures for $Na_{0.5}Bi_{0.5}Ti_{0.8}$ $Zr_{0.2}O_3$ ceramic. In the lower frequency side, normal variations in Z'' values with temperature and frequency were observed and all the curves at different temperatures appear to merge in to a single curve in the higher frequency region (figure 5 a & b). The reduction in Z" with increase in temperature below 200°C confirms PTCR behavior of the compound and above that NTCR behavior is observed. The shifting of the Z''_{max} in the direction of high frequency side in high temperature region is a consequence of relaxation phenomenon in the system. The reduction in resistance of grain when temperature rises is the cause of the shifting of peaks. Merging of all these curves at fusion frequency (f_f) is a symptom of the gathering of space charge in the studied compounds [21]. The low frequency region peak corresponds to grain boundary, while higher frequency region peak represents the bulk (grain) contribution. Decrement in peak height of the impedance spectra with rise in temperature is a characteristic feature very familiar in polycrystalline ceramics [22-24] which indicates temperature evolutions of relaxation processes. The value of resistance and capacitance for grain and grain boundary were obtained using the relation $2\pi f_m RC = 1$ from Z'' vs log f plot and indicating contributions from grain and grain boundary in the samples.

The figure 6 shows the plot of imaginary part M'' with frequency at different temperatures. The use of modulus

Table 2
Resistance (Rg, Rgb) and capacitance (Cg, Cgb) of grains and grain boundaries of $Na_{0.5}Bi_{0.5}Ti_{0.8}Zr_{0.2}O_3$ ceramics

Temperature (°C)	*Rg* (Ω)	*R*gb (Ω)	*C*g (F)	*C*gb (F)
400	1.128E+005	3.265E+002	5.015E-011	4.266E-010
425	6.652E+004	2.741E+002	5.071E-011	4.768E-010
450	3.707E+004	2.709E+002	5.249E-011	4.950E-010
475	1.668E+004	1.882E+002	4.476E-011	1.414E-009
500	9.821E+003	1.281E+002	5.670E-011	4.174E-010

spectroscopic plot is particularly useful for separating component with similar resistance but different capacitance. In figure 6, peaks appear to be shifted towards higher frequency side with rise in temperature. It is also observed that *M″* peaks broaden with decrease in temperature. The observed temperature and frequency dependence of *M″* arises due to distribution of relaxation time in the sample. The values of grain resistance (*R*g), grain boundary resistance (*R*gb), grain capacitance (*C*g) and grain boundary capacitance (*C*gb) are shown in table 2. The broadening of M" spectra must be intrinsically non-exponential process, like inter relationship among diffusion of the charged species, or diversities in the microstructure of the material, leading sequentially distribution of conduction of localized charged species in space and time to respond electrical effect.

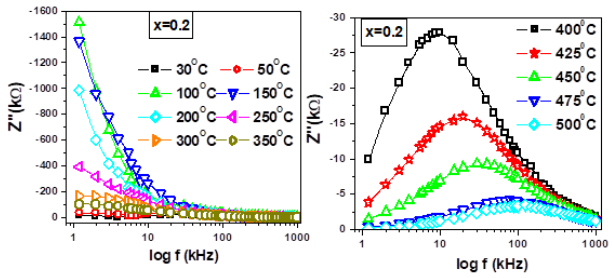

Fig. 5. (a) and (b): Frequency dependence of imaginary part of impedance Z″ at different temperatures for $Na_{0.5}Bi_{0.5}Ti_{0.8}Zr_{0.2}O_3$ ceramic sample

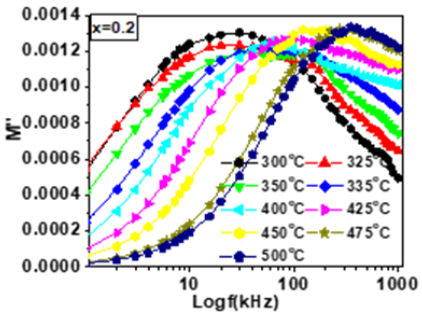

Fig. 6. Frequency dependence of imaginary part of modulus M″ at different temperatures for $Na_{0.5}Bi_{0.5}Ti_{0.8}Zr_{0.2}O_3$ ceramic sample

4. Conclusion

The polycrystalline sample of NBTZ was set up by a solid state-reaction route. Preliminary X-ray examination affirms the single phase orthorhombic crystal structure at room temperature. The plot solidly settled the ferro to paraelectric phase transition at 268˚C. Addition of Zr increases room temperature and peak dielectric constant values, which can be useful for dielectric for capacitor application. The dielectric constant of the ceramics diminishes with increasing frequency. Impedance and modulus spectroscopy reveals the presence of grain and grain boundary contribution in the sample. The activation energy of the compound was found to be distinctive in various regions demonstrating presence of various conduction components.

Acknowledgement

D. Panda acknowledges North Orissa University for the co-operation and help during his Ph.D research work. He extremely grateful to Director, PXE, Chandipur, for allowing him for the research programme. The authors are thankful to Prof. R.N.P. Choudhary, Professor, Department of Physics, ITER, Bhubaneswar who had helped us and permitted us to use his laboratory during synthesis of compound and some of analysis of its properties. D. Panda also acknowledges Department of Physics, Betnoti College Betnoti for allowing him to do some experimental work during his research.

References

[1] Mahajan S, Thakur O P and Prakash C 2009 J. Alloy Compds471 507.
[2] Mahajan S, Thakur O P, Bhattacharya D K and Sreenivas K 2008 Mater. Chem. Phys. 112 858.
[3] Mahajan S, Thakur O P, Bhattacharya D K and Sreenivas K 2009 J. Am. Ceram.. Soc. 92 416.
[4] Maiti T, Guo R and Bhalla A S 2006a Appl. Phys. Lett. 100 114109.
[5] Maiti T, Guo R and Bhalla A S 2006b Appl. Phys. Lett. 89 122909.
[6] Zhu, X.L., Chen, X.M., Liu, X.Q. and Yuan, Y. (2006) Dielectric Characteristics and Diffuse Ferroelectric Phase Transition in Sr4La2Ti4Nb6O30 Tungsten Bronze Ceramics. Journal of Materials Research, 21, 1787-1792.
[7] Huang, C., Bhalla, A.S. and Guo, R. (2005) Measurement of Microwave Electro-Optic Coefficient in Sr0.61Ba0.39Nb2O6 Crystal Fiber. Applied Physics Letters, 86.
[8] Ramirez, M.O., Jaque, D., Bausa, L.E., Sole Garci, J. and Kaminskii, A.A. (2005) Near Infrared and Visible Tunability from a Diode Pumped Nd Activated Strontium Barium Niobate Laser Crystal. Physical Review Letters, 95.
[9] Rao, K.S. and Nath, N.V. (2005) Influence of Rare-Earth Ion on Piezoelectric and Pyroelectric Properties of PBN System. Ferroelectrics, 325, 15-24.
[10] Jiang, W., Cao, W., Yi, X. and Chen, H. (2005) The Elastic and Piezoelectric Properties of Tungsten Bronze Ferroelectric Crystals (Sr0.7Ba0.3)2NaNb5O15 and (Sr0.3Ba0.7)2NaNb5O15. Journal of Applied Physics, 97,
[11] Raju, M.R. and Choudhary, R.N.P. (2006) Effect of Zr Substitution on Structural, Dielectric and Electrical Properties of Sr5SmTi3Nb7O30 Ceramics. Materials Chemistry and Physics, 99, 135-143.
[12] Chen, W., Kinemuchi, Y., Watari, K., Tamura, T. and Miwa, K. (2006) Preparation of Grain-Oriented Sr0.5Ba0.5Nb2O6 Ferroelectric Ceramics by Magnetic Alignment. Journal of the American Ceramic Society, 89, 381-384.
[13] Ko, H., Kojima, S., Lushnikov, S.G., Katiyar, R.S., Kim, T.-H. and Ro, J.-H. (2002) Low-Temperature Transverse Dielectric and Pyroelectric Anomalies of Uniaxial Tungsten Bronze Crystals. Journal of Applied Physics, 92, 1536.
[14] Wu, E. (1989) POWD, an Interactive Powder Diffraction Data Interpretation and Index Program. Ver.2.1. School of Physical Science, Flinders University South Bedford Park, Australia.
[15] Geiss, E.A., Scott, B.A., Burns, G., O'Kane, D.F. and Segmuller, A. (1969) Alkali Strontium-Barium-Lead Niobate Systems with a Tungsten Bronze Structure: Crystallographic Properties and Curie Points. Journal of the American Ceramic Society ,52, 276-281.
[16] Klug, H.P. and Alexander, L.E. (1974) X-Ray Diffraction Procedures for Polycrystalline and Amorphous Materials. Willey-Interscience, New York.
[17] Sahho, P.S., Panigrahi, A., Patri, S.K. and Choudhary, R.N.P. (2010) Impedance Spectroscopy of Ba3Sr2DyTi3V7O30 Ceramic. Bulletin of Materials Science, 33,129-134.
[18] Dash, S., Choudhary, R.N.P. and Kumar, A. (2014) Impedance Spectroscopy and Conduction Mechanism of Multiferroic

(Bi0.6K0.4)(Fe0.6Nb0.4)O3. Journal of Physics and Chemistry of Solids, 75, 1376-1382.
[19] Singh, A.K., Barik, S.K., Choudhary, R.N.P. and Mahapatra, P.K. (2009) Ac Conductivity and Relaxation Mechanism in Ba0.9Sr0.1TiO3. Journal of Alloys and Compounds, 479, 39-42.
[20] Bhattacharya, S., Bharadwaj, S.S.N. and Krupanidhi, S. B. (2000) Alternating Current Conduction Behavior of Excimer Laser Ablated SrBi2Nb2O9 Thin Films. Journal of Applied Physics, 88, 4294.